analytical chemistry

Article

pubs.acs.org/ac

Electrospray Ionization–Ion Mobility Spectrometry Identified Monoclonal Antibodies that Bind Exclusively to Either the Monomeric or a Dimeric Form of Prostate Specific Antigen

Robert C. Blake, II*,† and Diane A. Blake‡

†Division of Basic Pharmaceutical Sciences, College of Pharmacy, Xavier University of Louisiana, New Orleans, Louisiana 70125, United States

‡Department of Biochemistry and Molecular Biology, Tulane University School of Medicine, New Orleans, Louisiana 70112, United States

Supporting Information

ABSTRACT: Macroion mobility spectrometry was used to distinguish between a monoclonal antibody (clone M612165) that bound exclusively to monomeric prostate specific antigen and a different monoclonal antibody (clone M612166) that bound exclusively to a dimeric form of the antigen that only comprised 6.8% of the total protein. In the presence of excess antigen, the mobility spectrum of M612165 was replaced by a composite spectrum that represented a mixture of antibodies that included either one or two equivalents of the protein antigen. In similar circumstances, the mobility spectrum of M612166 was replaced by a composite spectrum that represented a mixture of antibodies that included either two or four equivalents of the protein antigen. When exposed to either of the two antibodies, the mobility spectrum of the prostate specific antigen showed a concomitant decrease in the monomeric antigen in one case and in the dimeric antigen in the other case. While sensitive kinetic exclusion assays demonstrated large differences in the antigen binding behavior of the two antibodies, these functional studies alone were insufficient to reveal the likely structural origins of the observed differences. Macroion mobility measurements were shown to be a useful and informative complement to functional studies in understanding complex macromolecular interactions.

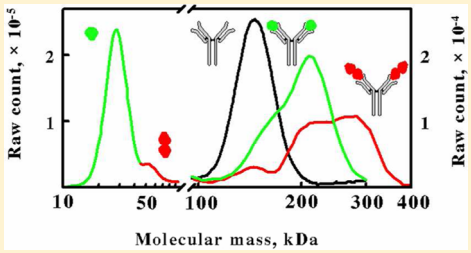

The development of electrospray ionization has led to powerful new tools for the study of proteins and protein complexes. Electrospray ionization techniques are now able to transfer macromolecules with masses over one million daltons into the gas phase.[1,2] Dilute solutions of proteins and protein oligomers,[3−8] nucleic acids,[9] ribosomes,[10] and small viruses[4,11,12] can be dispersed into droplets of 100−200 nm in diameter. Desolvation of these droplets generates highly charged particles that then pass through a neutralizing/charge reduction chamber[13] where they are converted into neutral and singly charged nanoparticles. The charged particles are then separated in the gas phase according to their electrophoretic mobility and quantified with a condensation particle counter. When the macromolecules are prepared in a physiological buffer amenable to electrospray (i.e., dilute ammonium acetate), even noncovalent protein complexes can be transferred intact to the gas phase.[2,14] This technology, variously referred to as electrospray ionization-ion mobility spectrometry (ESI-IMS),[1] nanoelectrospray gas-phase electrophoretic mobility molecular analysis (nES-GEMMA or GEMMA),[4] electrospray-differential mobility analysis (ES-DMA), or macroion mobility spectrometry (macroIMS),[15] was once available primarily to mass spectrometrists. However, complete instrument packages for macroIMS are available commercially and the technique is now accessible to any scientist with an interest in protein−protein interactions.

Our laboratories are focused on antibody-ligand interactions, and heretofore we have used the macroIMS technology primarily for quality control of our antibody preparations. MacroIMS has proven to be a simple and convenient method for analyzing the degree of proteolysis of our antibody preparations and for determining if antibody aggregation has occurred after storage. Monoclonal antibodies are the fastest growing sector in the pharmaceutics market today[16,17] and their aggregation can have unpredictable consequences, including the triggering of a severe or even life-threatening immune response in patients.[18,19] Bacher et al.[12] were the first to utilize macroIMS to study IgG aggregation and were able to resolve monomer, dimer, and trimers of bovine IgG. When compared with size-exclusion chromatography, analytical ultracentrifugation, and dynamic light scattering, macroIMS demonstrated superior resolving power in separating small percentages of dimers, trimers, and tetramers from main monomeric IgG peaks.[20] Further, macroIMS does not expose proteins to large solid−liquid interfaces, thereby avoiding the underestimation of aggregate levels as compared with size-exclusion chromatography.[20]

Received: June 4, 2012
Accepted: July 17, 2012
Published: July 17, 2012

In this study, we report the use of macroIMS to demonstrate that prostate specific antigen (PSA) can also exist as a dimer. The macroIMS technique was used to study the interaction of PSA and its dimer with two monoclonal antibodies that bind to PSA. The combination of macroIMS and kinetic exclusion analysis[21] revealed a heretofore unrecognized specificity of one of these monoclonal antibodies, that it bound preferentially to a PSA dimer. Analysis of binding data based on this newly characterized binding specificity helped resolve anomalous kinetic binding parameters reported previously for one of these antibodies.[22]

EXPERIMENTAL SECTION

Materials. Free prostate specific antigen that was purified from human seminal fluid and two purified mouse monoclonal antibodies directed against human PSA (clones M612165 and M612166) were purchased from Fitzgerald Industries, International (Concord, MA). Covalent conjugates of Cy5 and affinity-purified goat antimouse $(Fab)_2$-specific antibodies were obtained from Jackson ImmunoResearch Laboratories, Inc. (West Grove, PA). UltraLink Biosupport, an azlactone-activated beaded polyacrylamide resin (50−80 μM diameter), was purchased from Thermo Scientific (Rockford, IL). All other chemicals were reagent grade.

Kinetic Exclusion Assays. Kinetic exclusion assays were conducted using a KinExA 3000 flow fluorimeter purchased from Sapidyne Instruments, Inc. (Boise, ID). The general KinExA assay procedures are described in detail elsewhere.[21,23,24] All of the functional binding assays were conducted at 25 °C in Hepes-buffered saline (HBS), comprised of 137 mM NaCl, 3.0 mM KCl, and 10 mM Hepes, pH 7.4. The KinExA 3000 device is an immunoassay instrument that exploits an immobilized form of the antigen to separate and quantify the fraction of unoccupied binding sites that remain in reaction mixtures of antibody and antigen. The immobilized capture reagent for these studies consisted of PSA covalently coupled via its available lysine residues to azlactone-activated polyacrylamide beads. Dry amine-reactive beads (50 mg) were incubated with 1.0 mL of 100 μg/mL PSA in 0.085 M sodium carbonate, pH 9.5, for one hour at 25 °C. The beads were then washed three times with 1.0 mL of distilled water, and any remaining amine-reactive sites on the beads were blocked by incubation for two hours at 25 °C with 10 mg/mL bovine serum albumin in HBS amended with 0.03% (w/v) NaN_3. Beads could be stored in this blocking solution for up to two months at 4 °C. Immediately before use, the beads were diluted into 30 mL of HBS. The excess unreacted bovine serum albumin was washed away when individual aliquots of the PSA-coated beads were packed into the capillary observation cell of the KinExA 3000.

Reaction mixtures of antibody and antigen were incubated for at least one hour to achieve binding equilibrium before analysis. The fraction of occupied binding sites on the soluble anti-PSA was taken as

$$\text{fraction of occupied binding sites} = (\Delta F_0 - \Delta F_{exp})/(\Delta F_0 - \Delta F_{sat})$$

where ΔF is the observed difference in fluorescence readings at the beginning and the end of each experimental time course, and the subscripts 0, exp, and sat refer to instrumental time courses that correspond to a soluble PSA concentration of zero, an intermediate PSA concentration, and a saturating concentration of PSA, respectively. The value of the equilibrium dissociation constant, K_d, was obtained from a nonlinear regression fit of the following rectangular hyperbola to the data

$$\text{fraction of occupied binding sites} = [\text{PSA}]/([\text{PSA}] + K_d)$$

For kinetic studies, the fraction of unoccupied binding sites that remained after seven seconds of reaction was taken as

$$\text{fraction of binding sites remaining} = (\Delta F_{exp} - \Delta F_{sat})/(\Delta F_0 - \Delta F_{sat})$$

The value of the second order rate constant, k_{on}, for the bimolecular association between the soluble PSA and the antibody was obtained from a nonlinear regression fit of the following exponential function of the PSA concentration to the data[21]

$$\Delta F_{exp} = (\Delta F_0 - \Delta F_{sat})\exp(-k_{on}[\text{PSA}] \times 7s) + \Delta F_{sat}$$

The value of the corresponding unimolecular dissociation rate constant, k_{off}, for the antibody−antigen complex was obtained from the identity that $K_d = k_{off}/k_{on}$.

Macroion Mobility Measurements. Macroion mobility spectra of individual proteins and protein−protein complexes were obtained on a model 3980C macroIMS macroion mobility spectrometer from TSI, Inc. (Shoreview, MN). The instrument consisted of a model 3480 electrospray aerosol generator, a model 3080C electrostatic classifier, and a model 3776 macroion/nanoparticle detector. Protein samples from eight to 200 nM were prepared by diluting stock solutions that contained greater than 1.0 mg/mL protein into 20 mM ammonium acetate. Any nonvolatile salts that were present in the stock protein preparations were sufficiently diluted in the samples such that any spurious nonprotein peaks that were observed at low molecular masses did not interfere with the interpretation of the protein spectra. Control analyses using proteins that had been extensively dialyzed against 20 mM ammonium acetate, pH 7.4, demonstrated that neither the apparent masses nor the shapes of the resulting protein peaks in the macroIMS were changed by the desalting procedure. An example of such a comparison is shown in Figure S-1 in the Supporting Information. The ammonium acetate was prepared fresh weekly and passed through a 0.2 μm filter to remove any traces of particulate matter. If necessary, the pH of the solution was adjusted to 7.4 using either ammonium hydroxide or acetic acid.

Protein solutions for analysis were introduced as electrospray droplets by forcing the analyte through a fused silica capillary tube that terminated in a tip that was ground into a conical shape (available from TSI). The shape of the resulting source of emerging droplets was observed visually under magnification and controlled by adjusting the electrospray voltage and air pressure. The typical electrospray voltages ranged from 2.0 to 2.5 kV with currents ranging from 200 to 300 nA. The air around the spray tip entered the electrospray chamber at a rate of 1.5 L per minute; the capillary pressure differential was typically 3.5 to 4.0 PSID. The sheath flow rate was 20 L per minute; the flow rate into the condensation particle counter was 1.5 L per minute. Electrospray voltage and air pressure were adjusted until both the visible cone and the current were stable.

Multiply charged macroions that were included in the electrospray droplets then passed through a neutralizing/charge

dx.doi.org/10.1021/ac301527v | Anal. Chem. 2012, 84, 6899−6906

reduction chamber where they reacted with bipolar air molecules generated from a ^{210}Po alpha emitting source. Charge reduction changed the macroions into primarily neutral and singly charged macromolecules. Proteins and protein complexes were subsequently separated according to their mobilities in air and counted as a function of 128 discrete particle diameters from 4.78 to 15.1 nm by sweeping the voltage on the detector from 34 to 755 V. A protein particle density of 0.575/cm^3 was used to convert the particle diameters into the corresponding mass range of 2.5 to 600 kDas.[8] Each spectrum consisted of the accumulated counts of 10 repeat scans of 300 s each. The Sovitzky-Golay smoothing filter,[25] available in the MacroIMS operating software, was applied to the final spectrum using a sixth-order polynomial with three points on each side of the data point.

Spectra that represented mixtures of proteins or protein complexes were deconvoluted into sums of individual curves by iterative nonlinear regression analyses. Each suspected protein peak was modeled according to the distribution function

$$\text{counts} = A_1 + A_2 \times 4 \times \exp(-(X - A_3)/A_4)) / (1 + \exp(-(X - A_3)/A_4))^2$$

where X represents the molecular mass, A_1 is the average number of background counts, A_2 is the maximum number of counts at the highest point on that peak, A_3 is the molecular mass of that particular protein species, and A_4 represents the width of the peak at half-height. The overall mobility spectrum was then modeled as the sum of the individual distribution functions that represented each protein peak. Calculation of the parameter values (A_1 through A_n) that minimized the sum of the squares of the residual values between the observed and calculated values was accomplished using SlideWrite Plus for Windows (Advanced Graphic Software, Inc., Encinitas, CA).

RESULTS AND DISCUSSION

Antibody M612166 Bound Poorly to Immobilized Prostate Specific Antigen. The binding of PSA to an immobilized anti-PSA monoclonal antibody derived from clone M612166 was previously studied by 22 participants representing 13 institutions/companies.[22] Kinetic and equilibrium data were obtained using three different surface plasmon resonance platforms. The contents of the resulting 22 separate data sets were in remarkable agreement, indicating that the values of the second order rate constants for the bimolecular association of soluble PSA with the immobilized antibody were within 15% of 4.1×10^4 M^{-1} s^{-1}. However, this value was extremely low for an antibody–antigen binding interaction that would typically have a low energy of activation. For this reason, we wanted to reexamine this particular antibody–antigen binding reaction.

Initial kinetic exclusion assays conducted on the interaction of M612166 with PSA yielded observations that seemed to be consistent with the surface plasmon resonance data. Figure 1 shows examples of two different primary antibodies binding to immobilized PSA in a KinExA 3000 flow fluorimeter: curve a, 1.0 nM antibody M612166, and curve b, 0.5 nM antibody M612165, representing another anti-PSA monoclonal antibody that served as a comparative control for these experiments. Curve c in Figure 1 shows the instrumental response when no primary antibody was present in the analyte solution. The instrument response from 210 to 330 s represented the amount of primary antibody that was captured and retained on the immobilized PSA and was directly proportional to the

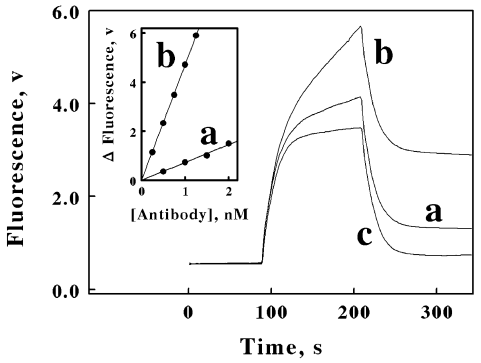

Figure 1. Examples of primary data collected on a KinExA 3000 flow fluorimeter for two different antibodies directed against prostate specific antigen. Selected time courses of individual fluorescence responses when beads bearing immobilized PSA were exposed in turn to mixtures of a primary mouse monoclonal antibody (0 to 90 s), fluorescently labeled goat antimouse antibodies (90 to 210 s), and a final buffer wash (210 to 330 s). Antibodies: *a*, 1.0 nM antibody M612166; *b*, 0.5 nM antibody M612165; and *c*, no primary antibody. Inset, secondary plot of the differences in the final fluorescence observed in the presence and absence of different concentrations of primary antibodies M612166 (*a*) or M612165 (*b*), respectively.

concentration of free antibody in solution (inset, Figure 1). The magnitudes of the instrumental responses obtained with antibody M612165 were typical of those that our laboratories have observed with other antibodies and immobilized antigens.[26−30] The magnitudes of the instrument responses obtained with antibody M612166 were much less than those obtained with other antibody–antigen pairs. There could be a number of explanations for the apparent poor binding of antibody M612166 to immobilized PSA, including, but not limited to, the following: the bimolecular association rate constant for the binding of the antibody to immobilized PSA is inherently low, as had been reported previously;[22] the antibody has a very poor affinity for the antigen; or the immobilized antigen is in the wrong conformation to promote rapid or high-affinity binding of the soluble antibody.

PSA Preparations Contained a Dimeric Contaminant. As part of an effort to understand why the binding of antibody M612166 to PSA appeared to be so poor, we subjected the highly purified protein reagents used in this study to macroion mobility spectrometry to independently assess their purity. The resulting spectrum for purified PSA is shown in Figure 2. The principal peak, centered at approximately 28 600 Da, clearly represented the purified free PSA. However, a minor contaminant with a higher molecular mass was always present in the same relative proportion in all spectra, regardless of the concentration of the total PSA preparation in the analyte solution. A clue as to the identity of this contaminant came from the analysis of the spectrum by nonlinear regression calculations. The observed spectrum was ably represented by the weighted sum of the contributions from two proteins, the major peak (93.2%) centered at 28 600 Da and a minor peak (6.8%) centered at 54 600 Da. Either this minor peak represented a structurally unrelated contaminant that was present in this highly purified PSA preparation, or the minor peak represented a stable dimeric form of the PSA. Although no evidence for the dimerization of PSA can be found in the literature, the 5 to 6% uncertainty in the absolute accuracy of macromolecular masses as determined by macroion mobility measurements[12] suggested that the minor peak could very well

dx.doi.org/10.1021/ac301527v | Anal. Chem. 2012, 84, 6899−6906

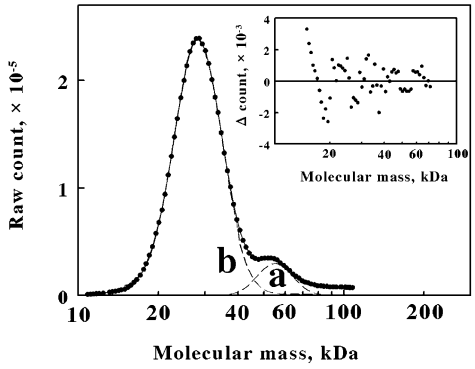

Figure 2. Macroion mobility spectrum of prostate specific antigen, demonstrating that the highly purified protein contained a dimeric contaminant. The parameters for the *solid curve* drawn through the data points were determined by nonlinear regression analysis using the sums of the calculated mobility spectra for two protein species with molecular masses of 54.6 and 28.6 kDa, representing *dashed curves a* and *b*, respectively. The area under *curve a* represents 6.8% of the total area under the *solid curve*. Inset, a residual plot of the differences between the observed and the calculated counts as a function of the molecular mass.

be an unexpected dimer of PSA. The possibility that the minor peak with the higher apparent mass simply represented the contents of droplets that coincidentally contained two unrelated monomers of PSA was discounted by two arguments. First, the concentration of total PSA, 200 nM, and the approximate volume of the individual droplets, 100 to 200 nL, dictated that these electrospray measurements were in the "one analyte per one droplet"[31] operating regime. Second, the relative proportion of the minor peak to the major peak did not change when the concentration of total PSA in the analyte solution was lowered as much as 10-fold below 200 nM. In addition, dilution of the protein samples did not cause the peaks to either shift to lower masses or change shape. Examples of macroIMS spectra obtained with different concentrations of PSA are shown in Figure S-2 in the Supporting Information.

Antibody M612165 Bound Exclusively to Monomeric PSA. The capacity for macroion mobility measurements to complement and extend the results of functional binding studies is illustrated in Figure 3. The binding of M612165 to PSA was determined by kinetic exclusion assays using equilibrium reaction mixtures comprised of a constant, limiting concentration of antibody M612165 and different concentrations of excess total PSA. The immobilized PSA in these assays was exploited to separate and quantify the fraction of soluble antibody binding sites that remained unoccupied in the equilibrium reaction mixtures of soluble antibody, antigen, and antibody–antigen complexes. Unlike surface plasmon resonance and other automated instrumentation devoted to the study of protein binding interactions in which the interaction to be quantified is that between a soluble and an immobilized binding partner,[32−34] the equilibrium binding data determined by kinetic exclusion assays are those obtained for the binding reaction in homogeneous solution. The equilibrium binding of total PSA to a limiting concentration of antibody M612165 is shown in Figure 3A. The rectangular hyperbola drawn through the data points in Figure 3A describes a one-site homogeneous binding reaction with an equilibrium dissociation constant of 5.6×10^{-8} M.

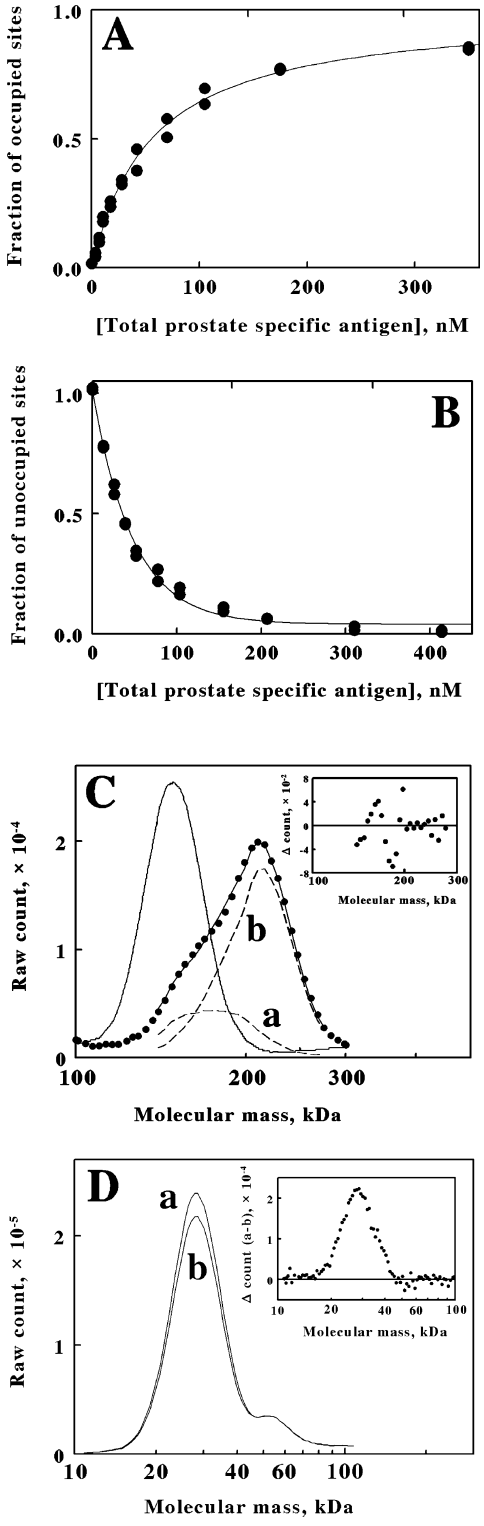

Figure 3. Monoclonal antibody M612165 bound monomeric prostate specific antigen. A, equilibrium data for the binding of PSA to the antibody. The parameters for the curve drawn through the data points were determined by nonlinear regression analysis using a one-site homogeneous binding model and a dissociation constant of 5.6×10^{-8} M. B, kinetic data for the binding of PSA to the antibody. Antibody (1.0 nM in binding sites) and PSA were incubated for 7 s before separation of the antibodies into bound and free fractions. The parameters for the curve drawn through the data points were determined by nonlinear regression analysis using a single exponential function of time and total PSA concentration and a value for the

dx.doi.org/10.1021/ac301527v | *Anal. Chem.* 2012, 84, 6899−6906

Figure 3. continued

bimolecular association rate constant of 2.8×10^6 $M^{-1}s^{-1}$. C, macroion mobility spectra of antibody M612165 (20 nM in binding sites) in the absence (*solid curve*) and presence (*solid curve* with *data points*) of 200 nM total PSA. The parameters for the *solid curve* drawn through the *data points* were determined by nonlinear regression analysis using the sum of the calculated mobility spectra for three proteins: 0.67 nM unliganded antibody with a mass of 150 kDas (not shown); 2.19 nM monoliganded antibody with a mass of 176 kDas (*dashed curve a*); and 7.14 nM diliganded antibody with a mass of 210 kDas (*dashed curve b*). Inset, a residual plot of the differences between the observed and the calculated counts as a function of the molecular mass. D, macroion mobility spectra of 200 nM total PSA in the absence (*a*) and presence (*b*) of 10 nM antibody M612165. Inset, difference spectrum representing the counts in *curve a* minus those in *curve b*. The peak of the difference spectrum occurs at 28.5 kDas.

Kinetic data for the bimolecular association of PSA with antibody M612165 are shown in Figure 3B. In this case, the reaction mixtures of limiting antibody and excess total PSA were only seven seconds old and far from equilibrium when the antibody molecules with unoccupied binding sites were separated from the reaction mixture and quantified using the immobilized PSA. The fraction of unoccupied binding sites was a single exponentially decreasing function of the total PSA concentration from which a second order rate constant of 2.8×10^6 M^{-1} s^{-1} was determined for the antibody–antigen binding reaction in solution.

Since the antibody–PSA complex had demonstrably greater mass than either the free antibody or the PSA alone, macroion mobility spectra were also conducted on antibody–antigen reaction mixtures to verify the anticipated masses and stoichiometries of different protein complexes that should be present. Figure 3C shows macroion mobility spectra for 10 nM antibody M612165 in the absence and presence of 200 nM total PSA. In the absence of antigen (solid curve), the antibody appeared as a single symmetrical peak (on the semilogarithmic plot) with no evidence for aggregated species or proteolytic breakdown products. In the presence of excess PSA (solid curve with data points), the resulting mobility spectrum was fit with a curve that represented the weighted sum of the curves of three proteinaceous species: 0.67 nM unliganded antibody at 150 kDas; 2.19 nM monoliganded antibody at 176 (150 + 26) kilodaltons (dashed curve *a*); and 7.14 nM diliganded antibody at 210 (150 + 60) kilodaltons (dashed curve *b*). These were the approximate concentrations and molecular masses that one would expect from a divalent antibody that independently bound two monomeric PSA molecules with an equilibrium dissociation constant of 5.6×10^{-8} M.

The data in Figure 3*D* show the macroion mobility spectra in the molecular mass range from 10 to 100 kDas for 200 nM total PSA in the absence (*curve a*) and presence (*curve b*) of 10 nM antibody M612165. The *inset* shows a difference spectrum of *curve a* minus *curve b*. The peak of the difference spectrum is centered at 28,000 Da. It was evident that the presence of antibody M612165 exclusively lowered the concentration of soluble monomeric PSA. The signal intensities in *curves a* and *b* were reliable quantitative measures of the PSA concentration. Control measurements showed that the area under each macroIMS spectrum was directly proportional to the PSA concentration in the analyte. Figure S-3 in the Supporting Information shows a standard curve of the total raw counts under each spectrum as a function of the concentration of PSA. The addition of antibody M612165 had no discernible effect on the concentration of the soluble higher mass contaminant in the PSA preparation.

Antibody M612166 Bound Exclusively to Dimeric PSA. The data in Figure 4 show the results of applying the same two complementary experimental methods to the binding of the same preparation of PSA to antibody M612166. The equilibrium binding of total PSA to a limiting concentration of antibody M612166 is shown in Figure 4A. The rectangular hyperbola (*solid line*) drawn through the data points in Figure 4*A* describes a one-site homogeneous binding reaction with an equilibrium dissociation constant of 5.7×10^{-8} M. The actual data points exhibited lower signal-to-noise characteristics than did the corresponding binding data in Figure 3*A*, but that is a likely consequence of the relatively poor capture of antibody M612166 compared with that of antibody M612165 on the immobilized PSA as discussed above for Figure 1. The *dashed curve* in Figure 4*A* represents a binding reaction with an equilibrium dissociation constant of 1.1×10^{-9} M, the value for the binding of PSA to antibody M612166 that was reported earlier using surface plasmon resonance measurements.[22] This graph illustrates that, when using the total concentration of PSA as the same basis for comparison, the values of the equilibrium dissociation constants for the same binding reaction as determined by kinetic exclusion assay and surface plasmon resonance differed by 5-fold.

Kinetic data for the bimolecular association of PSA with antibody M612166 are shown in Figure 4B. The fraction of unoccupied binding sites was a single exponentially decreasing function of the total PSA concentration from which a second order rate constant of 5.3×10^5 M^{-1} s^{-1} was determined for the antibody–antigen binding reaction in solution. The *dashed curve* in Figure 4B represents the equivalent progress of a binding reaction characterized by a second order rate constant of 4.1×10^4 M^{-1} s^{-1}, the value reported earlier for the binding of the same two reagents using surface plasmon resonance measurements.[22] Although the rate of PSA binding to antibody M612166 as determined by kinetic exclusion assay was an order of magnitude faster than that reported by surface plasmon resonance measurements, the higher value was still far slower than one might expect for a typical antibody–antigen binding interaction that could approach a diffusion-controlled transport limitation.

Figure 4C shows macroion mobility spectra in the molecular mass range from 100 to 500 kDas for 8.0 nM antibody M612166 in the absence and presence of 200 nM total PSA. In the absence of antigen (solid curve), antibody M612166 appeared as a single symmetrical peak with no evidence for aggregated species or proteolytic breakdown products. In the presence of excess protein antigen (solid curve with data points), new protein peaks appeared with molecular masses higher than those anticipated for an antibody that only bound one or two equivalents of monomeric PSA. The observed mobility spectrum in the presence of excess total PSA was fit with a curve that represented the weighted sum of the curves of the following three proteinaceous species: 0.74 nM unliganded antibody at 150 kDas; 1.98 nM antibody with a total mass of 205 kDas (*dashed curve a*); and 5.28 nM antibody with a total mass of 275 kDas (*dashed curve b*). The differences in mass

dx.doi.org/10.1021/ac301527v | *Anal. Chem.* 2012, 84, 6899–6906

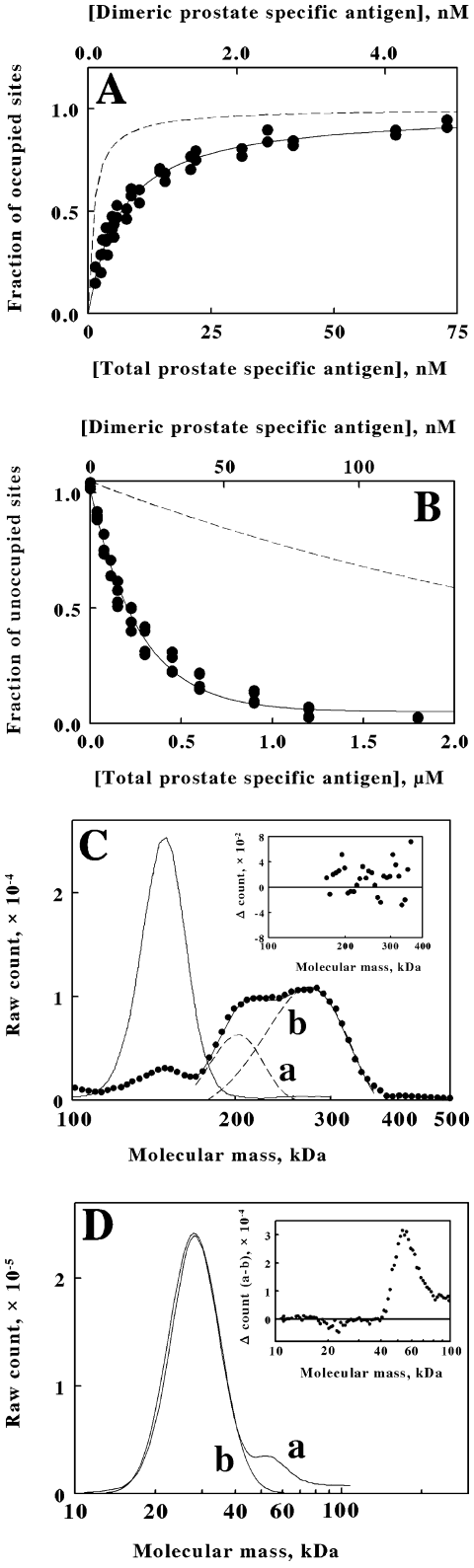

Figure 4. Monoclonal antibody M612166 bound dimeric prostate specific antigen. A, equilibrium data for the binding of PSA to the antibody. The parameters for the curve drawn through the data points were determined by nonlinear regression analysis using a one-site homogeneous binding model and dissociation constants for total and dimeric PSA of 5.7×10^{-8} and 3.9×10^{-10} M, respectively. B, kinetic data for the binding of PSA to the antibody. Antibody (5.0 nM in binding sites) and PSA were incubated for 7 s before separation of the antibodies into bound and free fractions. The parameters for the curve drawn through the data points were determined by nonlinear regression analysis using a single exponential function of time and total or dimeric PSA concentrations and values for the bimolecular association rate constants of 5.3×10^5 $M^{-1}s^{-1}$ or 7.8×10^6 $M^{-1}s^{-1}$, respectively. The values on the *upper X-axes* in A and B represent 6.8% of the values on the corresponding *lower X-axes*. The *dashed curves* in A and B represent the corresponding equilibrium and kinetic binding, respectively, of total PSA to antibody M612166 as determined elsewhere by surface plasmon resonance measurements. C, macroion mobility spectra of antibody M612166 (16 nM in binding sites) in the absence (solid curve) and presence (*solid curve* with *data points*) of 200 nM total PSA. The parameters for the *solid curve* drawn through the *data points* were determined by nonlinear regression analysis using the sum of the calculated mobility spectra for three proteins: 0.74 nM unliganded antibody with a mass of 150 kDas (not shown); 1.98 nM monoliganded antibody with a mass of 205 kDas (*dashed curve a*); and 5.28 nM diliganded antibody with a mass of 275 kDas (*dashed curve b*). *Inset*, a residual plot of the differences between the observed and the calculated counts as a function of the molecular mass. D, macroion mobility spectra of 200 nM total PSA in the absence (*a*) and presence (*b*) of 8.0 nM antibody M612166. *Inset*, difference spectrum representing the counts in *curve a* minus those in *curve b*. The peak of the difference spectrum occurs at 55.8 kDas.

between the unliganded antibody M612166 and each of the two new protein peaks, 55 and 125 kDas, were consistent with the hypothesis that antibody M612166 recognized and bound exclusively to the dimeric form of PSA that was present in the highly purified preparation. Thus the two new protein peaks with higher masses represented monoliganded and diliganded antibody where the ligand in question was dimeric PSA.

Further support for this hypothesis came from the macroion mobility spectra in the molecular mass range from 10 to 100 kDas for 200 nM PSA in the absence (*curve a*) and presence (*curve b*) of 8 nM antibody M612166, as illustrated in Figure 4*D*. The *inset* shows a difference spectrum of *curve a* minus *curve b*. The peak of the difference spectrum is centered at 55 800 Da. It was evident that the presence of antibody M612166 exclusively lowered the concentration of soluble dimeric PSA. The addition of antibody M612166 had no detectable effect on the concentration of the soluble monomeric PSA in the highly purified PSA preparation. It should be noted that no evidence was obtained that suggested that the monomeric PSA was in a facile or reversible equilibrium with the dimeric form. Thus the soluble dimeric PSA that was removed by binding to antibody M612166 was not rapidly replaced from the large pool of monomeric PSA as one would anticipate from the principle of mass action. Nor was the proportion of dimeric PSA dependent on the concentration of monomeric PSA over a 10-fold range in total PSA concentrations.

The realization that antibody M612166 bound exclusively to dimeric PSA prompted a reexamination of the equilibrium and kinetic data in Figures 4A and B, respectively. The *upper X-axes* in Figures 3A and B represent the concentration of dimeric PSA within the total PSA concentration represented on the corresponding *lower X-axes*. When analyzed on the basis of the concentration of dimeric PSA, the apparent equilibrium

dx.doi.org/10.1021/ac301527v | *Anal. Chem.* 2012, 84, 6899–6906

dissociation constant for the binding of dimeric PSA to antibody M612166 decreased from 5.7×10^{-8} to 3.9×10^{-10} M, while the value of the apparent second order rate constant for the bimolecular association of the two proteins increased from 5.3×10^5 M^{-1} s^{-1} to a more respectable value of 7.8×10^6 M^{-1} s^{-1}.

The combination of structural and functional studies presented herein provided for a much more insightful and powerful means of investigating the binding reaction than could have been achieved using either method alone. The published observation based on surface plasmon resonance measurements that the bimolecular association rate constant for the binding of antibody M612166 to PSA was only 4.1×10^4 M^{-1} s^{-1} should, perhaps, have prompted a further investigation as to why that value was so low. In the present study, the observations that (i) the capture and retention of soluble antibody M612166 by immobilized PSA was relatively ineffective and (ii) the value of the bimolecular second order rate constant for the soluble binding reaction was still unexpectedly low (5.3×10^5 M^{-1} s^{-1}) both prompted our further investigations into the possible structural origins of the unexpected functional behavior of monoclonal antibody M612166. It is evident that the macroion mobility studies complemented and extended the interpretation of the functional binding studies. Similarly, it is equally evident that the functional binding studies served to complement and extend the interpretation of the structural studies. Although we did not do so, it should be possible to obtain accurate equilibrium dissociation constants if macroion mobility spectra, such as those shown in Figures 3C and 4C were acquired at different concentrations of the excess protein antigen. Given the currently available instrumentation, it is not feasible to conduct kinetic binding studies using macroion mobility measurements. However, this study, which combined binding studies with measurements of the molecular masses of antibody−antigen complexes, together comprised a whole that was greater than the sum of its parts. Such an integrated approach may serve as a model for many other studies of protein−ligand interactions.

If one accepts the premise that antibody M612166 binds exclusively to a dimeric form of PSA, then one cannot simply go back and reinterpret the results of the prior surface plasmon resonance measurements[22] until one knows the percentage or concentration of the PSA dimer in the preparation used previously. The structural data on soluble PSA presented herein is only applicable to the characteristics of this one preparation. But the conclusion, that antibody M612166 binds exclusively to dimeric PSA, is presumably applicable to all preparations of the antibody. It is evident that the dimeric PSA presents a unique epitope that is not present or readily accessible in the properly folded monomeric PSA. Further research in our laboratories will examine the structural features of this dimeric PSA and how they differ from the monomeric PSA.

CONCLUSIONS

These data illustrate the advantages of incorporating both structural and functional measurements when investigating even relatively simple macromolecular binding interactions. Detailed functional studies, whether they are kinetic exclusion assays, surface plasmon resonance measurements, quartz crystal microbalance studies, isothermal titration calorimetry, or some other analytical means, can accurately characterize kinetic or equilibrium binding anomalies, but the same functional studies cannot necessarily provide data to eliminate various hypotheses to account for the source(s) of the apparent anomaly. In the present case, the macroion mobility measurements on the reactants and products of the binding reactions enabled us to propose simple, straightforward hypotheses that adequately accounted for the functional differences observed with the two different antibodies that bound the same protein antigen preparation. Further, the macroIMS measurements were performed relatively rapidly, and the resulting spectra were sensitive to small differences in mass and easily interpreted. There is no guarantee that we could have arrived at the same conclusions had we substituted analytical ultracentrifugation, flow field flow fractionation, gel filtration chromatography, or static/dynamic light scattering analyses for macroIMS measurements. The advantages of including macroIMS measurements in investigations of macromolecules and their interactions are evident.

ASSOCIATED CONTENT

Supporting Information

Three supplementary figures (Figures S-1 to S-3) that show additional macroIMS spectra. This material is available free of charge via the Internet at http://pubs.acs.org.

AUTHOR INFORMATION

Corresponding Author

*Tel: 504-5204789. Fax: 504-520-7954. E-mail: rblake@xula.edu.

Notes

The authors declare the following competing financial interest(s): RCB is on the Board of Directors of Sapidyne Instruments, Inc., a company that sells the KinExA 3000 flow fluorimeter that was used for part of this work. DAB declares no conflict of interest.

ACKNOWLEDGMENTS

This work was supported by Grants 5SC1AI081660-04 and 5G12RR026260-03 from the National Institutes of Health (RCB), and Grant DE-SC0004959 from the Office of Science within the U.S. Department of Energy (DAB).

REFERENCES

(1) Kaddis, C. S.; Loo, J. A. *Anal. Chem.* **2007**, *79*, 1778−1784.
(2) van den Heuvel, R. H.; Heck, A. J. *Curr. Opin. Chem. Biol.* **2004**, *8*, 519−526.
(3) Kaddis, C. S.; Lomeli, S. H.; Yin, S.; Berhane, B.; Apostol, M. I.; Kickhoefer, V. A.; Rome, L. H.; Loo, J. A. *J. Am. Soc. Mass Spectrom.* **2007**, *18*, 1206−1216.
(4) Allmaier, G.; Laschober, C.; Szymanski, W. W. *J. Am. Soc. Mass Spectrom.* **2008**, *19*, 1062−1068.
(5) Fernandez, d. l. M. J.; Ude, S.; Thomson, B. A. *Biotechnol. J.* **2006**, *1*, 988−997.
(6) van Duijn, E.; Bakkes, P. J.; Heeren, R. M.; van den Heuvel, R. H.; van Heerikhuizen, H.; van der Vies, S. M.; Heck, A. J. *Nat. Methods* **2005**, *2*, 371−376.
(7) van Duijn, E.; Barendregt, A.; Synowsky, S.; Versluis, C.; Heck, A. J. *J. Am. Chem. Soc.* **2009**, *131*, 1452−1459.
(8) Poderycki, M. J.; Kickhoefer, V. A.; Kaddis, C. S.; Raval-Fernandes, S.; Johansson, E.; Zink, J. I.; Loo, J. A.; Rome, L. H. *Biochemistry* **2006**, *45*, 12184−12193.
(9) van den Heuvel, R. H.; Gato, S.; Versluis, C.; Gerbaux, P.; Kleanthous, C.; Heck, A. J. *Nucleic Acids Res.* **2005**, *33*, e96.
(10) Hanson, C. L.; Fucini, P.; Ilag, L. L.; Nierhaus, K. H.; Robinson, C. V. *J. Biol. Chem.* **2003**, *278*, 1259−1267.

(11) Laschober, C.; Wruss, J.; Blaas, D.; Szymanski, W. W.; Allmaier, G. *Anal. Chem.* **2008**, *80*, 2261−2264.
(12) Bacher, G.; Szymanski, W. W.; Kaufman, S. L.; Zollner, P.; Blaas, D.; Allmaier, G. *J. Mass Spectrom.* **2001**, *36*, 1038−1052.
(13) Scalf, M.; Westphall, M. S.; Krause, J.; Kaufman, S. L.; Smith, L. M. *Science* **1999**, *283*, 194−197.
(14) Catalina, M. I.; van den Heuvel, R. H.; van Duijn, E.; Heck, A. J. *Chem.—Eur. J.* **2005**, *11*, 960−968.
(15) Carazzone, C.; Raml, R.; Pergantis, S. A. *Anal. Chem.* **2008**, *80*, 5812−5818.
(16) Beck, A.; Haeuw, J. F.; Wurch, T.; Goetsch, L.; Bailly, C.; Corvaïa, N. *Discovery Med.* **2010**, *10*, 329−339.
(17) Reichert, J. M. *mAbs* **2011**, *3*, 76−99.
(18) Braun, A.; Kwee, L.; Labow, M. A.; Alsenz, J. *Pharm. Res.* **1997**, *14*, 1472−1478.
(19) Wang, W. *Int. J. Pharm.* **2005**, *289*, 1−30.
(20) Mahler, H. C.; Jiskoot, W. In *Analysis of Aggregates and Particles in Protein Pharmaceuticals*; John Wiley & Sons, Inc.: Hobokan, NJ, 2012; pp 133−152.
(21) Blake, R. C., II; Pavlov, A. R.; Blake, D. A. *Anal. Biochem.* **1999**, *272*, 123−134.
(22) Katsamba, P. S.; Navratilova, I.; Calderon-Cacia, M.; Fan, L.; Thornton, K.; Zhu, M.; Bos, T. V.; Forte, C.; Friend, D.; Laird-Offringa, I.; Tavares, G.; Whatley, J.; Shi, E.; Widom, A.; Lindquist, K. C.; Klakamp, S.; Drake, A.; Bohmann, D.; Roell, M.; Rose, L.; Dorocke, J.; Roth, B.; Luginbühl, B.; Myszka, D. G. *Anal. Biochem.* **2006**, *352*, 208−221.
(23) Blake, D. A.; Chakrabarti, P.; Khosraviani, M.; Hatcher, F. M.; Westhoff, C. M.; Goebel, P.; Wylie, D. E.; Blake, R. C., II *J. Biol. Chem.* **1996**, *271*, 27677−27685.
(24) Blake, II, R. C.; Blake, D. A. In *Antibody Engineering: Methods and Protocols*; Methods in Molecular Biology Vol. *248*; Lo, B. K. C., Ed.; Humana Press, Inc.: Totowa, NJ, 2003; pp 417−430.
(25) Savitsky, A.; Golay, M. J. E. *Anal. Chem.* **1964**, *36*, 1627−1639.
(26) Blake, R. C., II; Li, X.; Yu, H.; Blake, D. A. *Biochemistry* **2007**, *46*, 1573−1586.
(27) Blake, II, R. C.; Ohmura, N.; Lackie, S. J.; Delehanty, J. B.; Darwish, I. A.; Blake, D. A. In *Trends in Monoclonal Antibody Research*; Simmons, M. A., Ed.; Nova Science Publishers, Inc.: Hauppauge, NY, 2005; pp 1−35.
(28) Blake, R. C., II; Pavlov, A. R.; Khosraviani, M.; Ensley, H. E.; Keifer, G. E.; Yu, H.; Li, X.; Blake, D. A. *Bioconjugate Chem.* **2004**, *15*, 1125−1136.
(29) Blake, R. C., II; Delehanty, J. B.; Khosraviani, M.; Yu, H.; Jones, R. M.; Blake, D. A. *Biochemistry* **2003**, *42*, 497−508.
(30) Khosraviani, M.; Blake, R. C., II; Pavlov, A. R.; Lorbach, S. C.; Yu, H.; Delehanty, J. D.; Brechbiel, M. W.; Blake, D. A. *Bioconjugate Chem.* **2000**, *11*, 267−277.
(31) Hogan, C. J., Jr.; Biswas, P. *J. Am. Soc. Mass Spectrom.* **2008**, *19*, 1098−1107.
(32) Baird, C. L.; Myszka, D. G. *J. Mol. Recognit.* **2001**, *14*, 261−268.
(33) Smith, R. H.; Lemon, W. J.; Erb, J. L.; Erb-Downward, J. R.; Downward, J. G.; Ulrich, O. E.; Wittliff, J. L. *Clin. Chem.* **1999**, *45*, 1683−1685.
(34) Becker, B.; Cooper, M. A. *J. Mol. Recognit.* **2011**, *24*, 754−787.